# Supporting Information

# Secondary Doping of Mn/Co Bimetallic ZIF-derived Catalysts for Oxygen Reduction Reactions

Lingli Guo, Yuekun Hu, Xiaowei Zhao, Xingkai Peng, Xinghua Zhang, Xiaofei Yu, Xiaojing Yang, Zunming Lu, Lanlan Li*

*School of Materials Science and Engineering, Hebei University of Technology, Tianjin 300130, China*

*Corresponding Author. E-mail addresses: liabc@hebut.edu.cn (L.L. Li)

## Experimental Details

### Chemicals

Zinc acetate $(CH_3COO_2)Zn\cdot 2H_2O$, cobalt nitrate hexahydrate $(Co(NO_3)_2\cdot 6H_2O$, manganese（II） acetate tetrahydrate $Mn(CH_3COO)_2\cdot 4H_2O$ and 2-methylimidazole (2-MIM). The commercial Pt/C (Com. Pt/C) catalyst is 20 wt.% of ~3 nm Pt nanoparticles on Vulcan XC-72 carbon support. Nafion was acquired from Sigma-Aldrich. All chemicals were used as received without any further purification.

### Electrochemical measurements

Cyclic voltammetry (CV) was carried out in a nitrogen ($N_2$) or oxygen ($O_2$) saturated electrolyte (0.1 M KOH or 0.1 M $HClO_4$) with a scan rate of 50 mV $s^{-1}$. Linear sweep voltammetry (LSV) curves were measured in an $O_2$-saturated electrolyte (0.1 M KOH or 0.1 M $HClO_4$) through the RDE method at 1600 rpm with a scan rate of 10 mV $s^{-1}$. Tafel slopes were calculated as follows:

$$\eta = a + b\log\left(\frac{j}{j_0}\right) \#(1)$$

where η, b, j, and $j_0$ are the overpotential, the Tafel slope, the current density, and the exchange current density, respectively.

Also, the ORR diffusion kinetics and electron transfer number (n) were studied according to the Koutecky-Levich equations by measuring the diffusion-limiting currents at different rotation speeds ranging from 400 to 2025 rpm. The n and kinetic current density ($J_k$) were calculated from Koutecky-Levich equation at various electrode potential:

$$\frac{1}{J} = \frac{1}{J_L} + \frac{1}{J_K} = \frac{1}{B\omega^{\frac{1}{2}}} + \frac{1}{J_K}\#(2)$$

$$B = 0.2nFC_0D_0^{\frac{2}{3}}V^{-\frac{1}{6}}\#(3)$$

where J, $J_K$ and $J_L$ are the measured current density, the kinetic current density and the diffusion-limiting current density, respectively; ω is the angular velocity; n and F is the electron transfer number and the Faraday constant (96485 C $mol^{-1}$); $C_0$ and $D_0$ are the bulk concentration of $O_2$ ($1.2 \times 10^{-6}$ mol $cm\text{-}^{3}$) and the diffusion coefficient of $O_2$ ($1.9\times10^{-5}$ $cm^2$ $s^{-1}$); V is the kinematic viscosity of the electrolyte (0.01 $cm^2$ $s^{-1}$). The constant 0.2 is adopted when the rotation speed is expressed in rpm.

The four-electron selectivity of catalysts was assessed based on the $H_2O_2$ yield. The $H_2O_2$ yield and the n were determined by the following equations:

$$H_2O_2(\%) = 200\frac{\frac{I_r}{N}}{I_d + \frac{I_r}{N}}\#(4)$$

$$n = 4\frac{I_d}{I_d + \frac{I_r}{n}}\#(5)$$

where $I_d$ is disk current, $I_r$ is ring current, N is current collection efficiency of the Pt ring, and was determined to be 0.40. Electrochemical impedance spectroscopy (EIS) was carried out from 100 kHz to 0.01 Hz at the 0.85 V (vs. RHE) potential with an amplitude of 5 mV.

The accelerated dur-ability tests (ADTs) of the as-synthesized catalysts and Com. Pt/C were performed in all the $O_2$-saturated electrolytes (0.1 M KOH or 0.1 M $HClO_4$) at room temperature by potential cycling ranging from for 20 000 cycles. At the end of cycling, the final catalyst-loaded working electrode was subjected to polarization measurement, highlight the difference of half-wave potential($E_{1/2}$) for catalysts before and after 5 000 cycles. Fixed voltage of 0.50 V (vs. RHE) to the working electrode, the stability of the catalyst was analyzed by Chronoamperometry to record the change in current intensity with test time (I-t) and to analyze the stability of the catalyst.

In addition, methanol tolerance of the catalysts was tested by conducting the ORR in the presence of methanol (1M) in $O_2$-saturated electrolytes of 0.1 M KOH or 0.1 M $HClO_4$ by chronoamperometric measurements."

Supplementary Figures and Tables

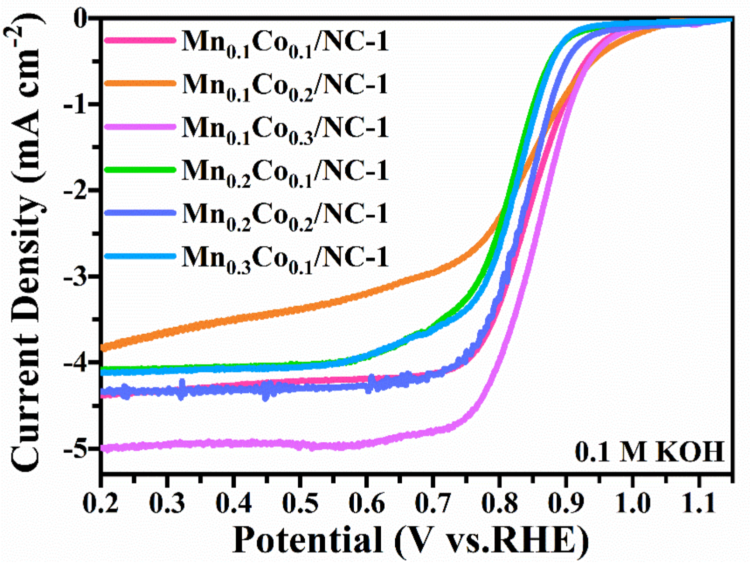


Fig. S1 LSV curves of catalysts with different Mn, Co molar ratios

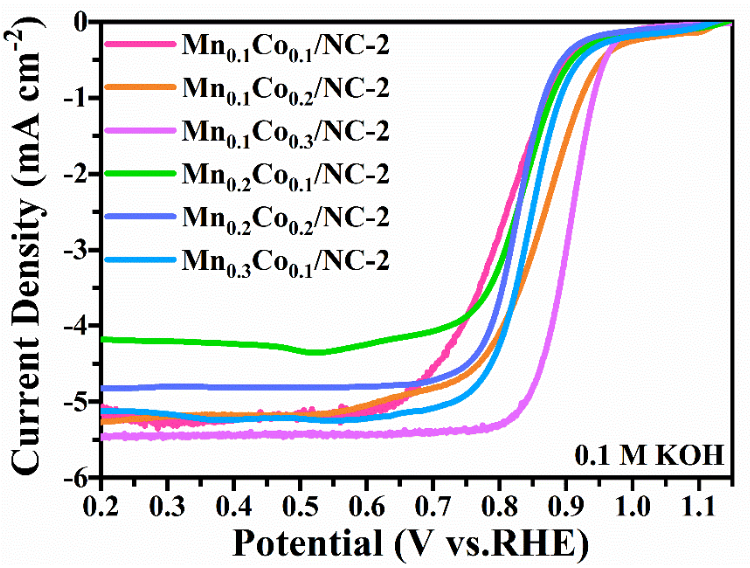


Fig. S2 LSV curves of secondary doping of catalysts

Table. S1 Elemental quantification（at%）determined by XPS of $Mn_{0.4}$/NC-2, $Mn_{0.1}Co_{0.3}$/NC-1, $Mn_{0.1}Co_{0.3}$/NC-2 and $Co_{0.4}$/NC-2

| Samples | C | N | Mn | Co |
|---|---|---|---|---|
| $Mn_{0.4}$/NC-2 | 87.25 | 12.58 | 0.57 | |
| $Mn_{0.1}Co_{0.3}$/NC-2 | 87.59 | 12.04 | 0.15 | 0.22 |
| $Mn_{0.1}Co_{0.3}$/NC- 2 | 86.84 | 12.52 | 0.28 | 0.36 |
| $Co_{0.4}$/NC-2 | 87.41 | 12.19 | | 0.4 |

Table. S2 The peak fitting of N 1s XPS data of $Mn_{0.4}$/NC-2, $Mn_{0.1}Co_{0.3}$/NC-1, $Mn_{0.1}Co_{0.3}$/NC-2 and $Co_{0.4}$/NC-2

| Samples | $M-N_x$ (%) (399.3 eV) | $M-N_x$ (at%) |
|---|---|---|
| $Mn_{0.4}$/N/C-2 | 11.18 | 1.41 |
| $Mn_{0.1}Co_{0.3}$/NC-1 | 10.15 | 1.22 |
| $Mn_{0.1}Co_{0.3}$/NC-2 | 16.56 | 2.07 |
| $Co_{0.4}$/NC-2 | 12.23 | 1.49 |

Table. S3 $E_0$ and $E_{1/2}$ for different amounts of Mn and Co first doping catalysts

| Samples | $E_0$ (V) | $E_{1/2}$ (V) |
|---|---|---|
| $Mn_{0.1}Co_{0.1}$/NC-1 | 0.959 | 0.848 |
| $Mn_{0.1}Co_{0.2}$/NC-1 | 0.961 | 0.841 |
| $Mn_{0.1}Co_{0.3}$/NC-1 | 0.975 | 0.859 |
| $Mn_{0.2}Co_{0.1}$/NC-1 | 0.903 | 0.829 |
| $Mn_{0.2}Co_{0.2}$/NC-1 | 0.932 | 0.846 |
| $Mn_{0.3}Co_{0.1}$/NC-1 | 0.901 | 0.832 |

Table. S4 $E_0$ and $E_{1/2}$ for different amounts of Mn and Co secondary doping catalysts

| Samples | $E_0$ (V) | $E_{1/2}$ (V) |
|---|---|---|
| $Mn_{0.1}Co_{0.1}$/NC-2 | 0.928 | 0.803 |
| $Mn_{0.1}Co_{0.2}$/NC-2 | 0.950 | 0.859 |
| $Mn_{0.1}Co_{0.3}$/NC-2 | 0.985 | 0.903 |
| $Mn_{0.2}Co_{0.1}$/NC-2 | 0.933 | 0.847 |
| $Mn_{0.2}Co_{0.2}$/NC-2 | 0.919 | 0.835 |
| $Mn_{0.3}Co_{0.1}$/NC-2 | 0.948 | 0.849 |